IEEE Access
Multidisciplinary | Rapid Review | Open Access Journal

Received September 10, 2019, accepted October 8, 2019, date of publication October 14, 2019, date of current version October 25, 2019.

Digital Object Identifier 10.1109/ACCESS.2019.2947238

Smart Home Energy Management in Unbalanced Active Distribution Networks Considering Reactive Power Dispatch and Voltage Control

DAVYE MAK, (Student Member, IEEE), AND DAE-HYUN CHOI, (Member, IEEE)
School of Electrical and Electronics Engineering, Chung-Ang University, Seoul 156-756, South Korea

Corresponding author: Dae-Hyun Choi (dhchoi@cau.ac.kr)

This work was supported in part by the National Research Foundation of Korea (NRF) grant funded by the Korean Government (MSIP) under Grant 2018R1C1B6000965, in part by the Human Resources Development of the Korea Institute of Energy Technology Evaluation and Planning (KETEP) grant funded by the Korea Government Ministry of Trade, Industry and Energy under Grant 20184030202070, and in part by the Ministry of Science and ICT (MSIT), South Korea, under the Information Technology Research Center (ITRC) support program supervised by the Institute for Information & Communications Technology Planning & Evaluation (IITP) under Grant IITP-2019-2018-0-01799.

ABSTRACT This paper presents a new optimization algorithm for home energy management systems (HEMSs) in three-phase unbalanced low-voltage (LV) distribution networks. Compared with conventional HEMS optimization methods, which consider only the active power consumption scheduling for smart home appliances and distributed energy resources (DERs) (e.g., solar photovoltaic (PV) systems and energy storage systems (ESSs)), the novelty of the proposed approach is to consider: i) both active and reactive power consumption schedulings of home appliances and DERs, ii) realistic three-phase unbalanced LV distribution networks with voltage-dependent load models, and iii) voltage control using an on-load tap changer transformer and smart inverters of PV system and ESS at the households. The proposed HEMS optimization algorithm, which is formulated using mixed-integer linear programming, is tested in the modified CIGRE LV distribution network. Numerical examples demonstrate the performance of the proposed algorithm in terms of active/reactive power consumption, three-phase voltage magnitudes, and the total cost of electricity.

INDEX TERMS Home energy management, smart household appliance, three-phase unbalanced distribution system, reactive power dispatch, voltage control, voltage dependent load.

NOMENCLATURE

The main notations used throughout this paper are summarized here. Bold symbols represent vectors or matrices. Hat symbols represent estimates of true parameter value. Other undefined symbols are explained within the text.

SETS

$\mathcal{U}$	Set of nodes in LV distribution network.
$\mathcal{L}$	Set of branches in LV distribution network.
$\mathcal{T}$	Set of scheduling horizon with one-hour resolution.
Φ	Set of phases of three-phase lines or nodes.
$\mathcal{D}_v$	Set of nodes that are connected downstream from node v.
$\mathcal{N}^{\text{Tap}}$	Set of tap positions corresponding to turn ratio of an on-load tap changer transformer.

VARIABLES

$P^{\text{net}}_{u,t}$	Net active power consumption of household u at time t.
$P^{\text{sell}}_{u,t}$	Net active power supply to grid by household u at time t.
$\delta_{u,t}$	Discomfort cost of household u at time t.
$P(Q)^{\text{load}}_{u,t}$	Total active(reactive) load power consumption of household u at time t.
$P^{\text{ESS,ch(dch)}}_{u,t}$	ESS charging(discharging) power of household u at time t.
$P^{\text{ESS,home,dch}}_{u,t}$	ESS active power discharge of household u at time t for supplying household load.

The associate editor coordinating the review of this manuscript and approving it for publication was Bin Zhou.

$P_{u,t}^{\mathrm{ESS,sell,dch}}$ ESS active power discharge of household u at time t for supplying grid.
$P_{u,t}^{\mathrm{PV,home}}$ PV active power of household u at time t for supplying household load.
$P_{u,t}^{\mathrm{PV,sell}}$ PV active power of household u at time t for supplying grid.
$P(Q)_{uv,t}^{\mathrm{line}}$ Active(reactive) power flow in line uv at time t.
$P(Q)_{u,t}^{\mathrm{node}}$ Nodal active(reactive) power of household u at time t.
$P(Q)_{u,t}^{\mathrm{c}}$ Active(reactive) power consumption of of controllable load of household u at time t.
$SOC_{u,t}$ ESS state-of-charge of household u at time t.
$T_{u,t}^{\mathrm{in}}$ Indoor temperature of household u at time t.
$b_{u,t}^{\mathrm{net}}$ Binary variable for ensuring power trading status of household u at time t.
$b_{u,t}^{\mathrm{ESS}}$ Binary variable for specifying ESS charging and discharging status of household u at time t.
$Q_{u,t}^{\mathrm{PV}}$ Injected/absorbed reactive power from PV system of household u at time t.
$Q_{u,t}^{\mathrm{ESS}}$ Injected/absorbed reactive power from ESS of household u at time t.
$V_{u,t}^{\mathrm{sq}}$ Vector of square of voltage magnitudes for three phases at node u at time t.
$P(Q)_{u,t}^{\mathrm{load,nom}}$ Active(reactive) power consumption of household u at time t at nominal voltage.
$a_{\phi,t}^{\mathrm{OLTC,sq}}$ Square of OLTC turn ratios for each phase at time t.
$U_{\phi,t,i}^{\mathrm{Tap}}$ Binary variable for determining a proper turn ratio of OLTC of phase ϕ at time t.

PARAMETERS

$\pi_t^{\mathrm{buy(sell)}}$ TOU-based buying(selling) price from(to) grid at time t.
ϵ_u Penalty parameter of discomfort cost of household u.
$\widehat{P}_{u,t}^{\mathrm{PV}}$ Predicted PV active power output of household u at time t.
$\eta_u^{\mathrm{ch(dch)}}$ ESS charging(discharging) efficiency of household u.
$E_u^{\mathrm{ESS,max}}$ Maximum ESS capacity of household u.
$\widehat{T}_{u,t}^{\mathrm{out}}$ Predicted outdoor temperature of household u at time t.
$SOC_u^{\mathrm{min(max)}}$ Minimum(maximum) ESS state-of-charge of household u.
$P_u^{\mathrm{ESS,ch,min}}$ Minimum ESS charging active power of household u.
$P_u^{\mathrm{ESS,ch,max}}$ Maximum ESS charging active power of household u.
$P_u^{\mathrm{ESS,dch,min}}$ Minimum ESS discharging active power of household u.
$P_u^{\mathrm{ESS,dch,max}}$ Maximum ESS discharging active power of household u.
$T_u^{\mathrm{min(max)}}$ Minimum(maximum) indoor temperature of household u.
$P_u^{\mathrm{c,min(max)}}$ Minimum(maximum) controllable load active power consumption of household u.
δ_u^{max} Maximum relaxation variable of discomfort cost of household u.
$P(Q)_{u,t}^{\mathrm{uc}}$ Predicted active(reactive) power consumption of uncontrollable loads of household u at time t.
$Q_{u,\phi}^{\mathrm{PV,min(max)}}$ Minimum(maximum) PV reactive power capacity of household u at phase ϕ.
$Q_{u,\phi}^{\mathrm{ESS,min(max)}}$ Minimum(maximum) ESS reactive power capacity of household u at phase ϕ.
$V^{\mathrm{min(max),sq}}$ Square of minimum(maximum) voltage magnitude in the system.
$V^{\mathrm{nom,sq}}$ Square of nominal value of voltage magnitude in the system.

I. INTRODUCTION

As residential households consume approximately one third of the total electricity consumption [1], home energy management systems (HEMSs) have become an indispensable technology for the efficient and economical management of residential energy usage. The primary goal of the conventional HEMS is to reduce consumers' electricity costs in their comfortable and preferred environments by scheduling the optimal energy consumption of smart household appliances (e.g., air conditioners and washing machines).

Recently, emerging smart grid technologies including distributed energy resources (DERs) (e.g., rooftop solar photovoltaic (PV) and energy storage system (ESS)), advanced metering infrastructure with smart meters, and demand side management have enabled consumers to achieve more energy saving through the HEMSs equipped with these smart grid technologies [2]. A core technology for the conventional HEMS is the optimization method employed to conduct an economic load reduction and load shifting of smart household appliances in addition to the operation scheduling of the DERs (e.g., charge/discharge of the ESSs).

However, the conventional HEMS optimization algorithm may calculate the incorrect and undesired energy consumption schedules for smart households due to the the following limitations. First, only the scheduling of active power consumption of household appliances and active power injection/absorption of the DERs is considered excluding reactive power consumption of appliances along with reactive power capability of the DERs. Second, the conventional HEMS algorithm is designed assuming houses are connected to three-phase balanced low-voltage (LV) distribution systems. However, the LV distribution systems are naturally unbalanced where the load consumptions on each phase are always changing independently [3]. Lastly, only constant power load models excluding load-voltage dependency in households are incorporated into the conventional HEMS optimization formulation. Indeed, the consumer load varies

along with voltage and is generally formulated as the static polynomial ZIP load model [4] where Z, I, and P represent constant impedance load, constant current load, and constant power load, respectively. In this environment, the conventional HEMS approach neglects the voltage quality for the individual consumer, and does not consider the impact of Volt-VAR optimization (VVO) through a voltage regulating device (e.g., an on-load tap changer (OLTC)) [5] or voltage control capability and reactive power dispatch of the DERs [6], [7] on the HEMS performance.

Conservation voltage reduction (CVR) is one of the main applications of VVO in distribution management systems. The CVR method is a cost efficient solution, which lowers distribution voltages to allow for consumer energy savings and peak demand reduction while keeping consumer voltages above the minimum operating limits through the coordination of an OLTC, capacitor banks, and the smart inverters of DERs [8]. Much research has focused on the development of the CVR and VVO methods and the assessment of their impact on distribution grid operations and energy savings in the following three schemes. In the centralized approach, using mixed-integer nonlinear programming, day-ahead models with voltage regulating devices [9] and model predictive control-based approaches were formulated by considering solar PV and wind turbine generators [10]. In the hierarchical distributed approach, in unbalanced three-phase distribution systems, algorithms to reduce the computational burden have been proposed based on the alternating direction method of multipliers [11] and a two-stage optimization problem [12]. In the fully distributed approach, an inverter-based model-free VVO scheme has been proposed, in which each local agent is coordinated with each other to adjust their reactive power and curtail the active power in order to alleviate overvoltage phenomena [13]. Concise summaries of implementation strategies, evaluation methods, and practical applications of CVR were presented in [14]. Considering the energy savings obtained from CVR, the HEMS integrated with CVR may provide more energy savings with consumers than the conventional HEMS.

To address the aforementioned limitations and challenges, this study proposes a more practical HEMS optimization algorithm that can be executed in realistic distribution system operating conditions. Specifically, in three-phase unbalanced LV distribution networks, the proposed approach schedules the optimal consumption of both active and reactive power of unbalanced voltage-dependent household loads to reduce the electricity cost within the consumers comfort level while maintaining voltage quality along the distribution feeders by the operation of OLTCs and the active and/or reactive power dispatch of the DERs.

A number of researchers have reported methods to manage home energy consumption. HEMS algorithms considering the physical load model for home appliances were proposed and executed based on load priority and consumers' comfort level [15], [16]. Over the last decade, considerable effort has been devoted to formulating HEMS algorithms in different types of optimization models [17]–[28], ranging from the scheduling of different types of home appliances along with electric vehicles using linear programming (LP) [17], [18], load scheduling considering the consumers' comfort level using mixed integer nonlinear programming (MINLP) [19], a convex programming based on relaxed MINLP using an L_1 regularization technique [20], load scheduling for multiple consumers using mix-integer linear programming (MILP) [21], [22], LP-based joint optimization of energy supplies and electric loads through three-stage scheduling (prediction, supply control, and demand control) [23], natural aggregation algorithm (NAA)-based HEMS method consisting of forecasting, day-ahead scheduling, and actual operation [24], robust optimization for the scheduling of home appliances to resolve the uncertainty of consumer behavior [25] and outdoor temperature and consumers' comfort level [26], and distributed HEMS architectures consisting of a local HEMS and global HEMS [27], [28]. The previous work on the HEMS algorithms including different types of optimization models is summarized well in [29].

Compared to the extensive research on HEMS optimization algorithms, only limited studies have investigated the relationship between HEMS scheduling and the actual distribution system operating conditions. A co-simulation platform was developed to assess the physical and economic impact of a HEMS under different time-of-use (TOU) pricing schemes on distribution systems in [30]. In [31], a bi-level optimization problem was formulated to quantify the impact of demand response (DR) from a HEMS on the voltage profile. A HEMS algorithm based on voltage control was proposed to maximize consumers' comfort level by controlling household passive loads [32]. In [33], considering voltage-dependent load models, demand response mismatch (DRM) (i.e., an active power mismatch between the scheduled and actually achieved DR) was introduced, and the MINLP optimization problem was formulated to minimize the DRM.

However, a considerable portion of the recent research on HEMS optimization methods has assumed unrealistic distribution system models and operating conditions without explicitly considering: i) active and reactive power consumption in the voltage-dependent load model, ii) active and/or reactive power dispatch of DERs with OLTC operation for voltage control, and iii) three-phase unbalanced distribution feeders and load models. Prior work [30]–[33] investigated the interaction between HEMSs with DR-enabled household appliances and physical distribution system conditions such as reactive power and voltage quality. However, no realistic and practical HEMS optimization method to resolve the challenges above has been proposed to date.

The novelty of this paper is that it provides a practical HEMS optimization framework that schedules the economical energy consumption of smart household appliances based on three-phase unbalanced voltage-dependent load models, considering the control of the OLTC and DERs to

provide consumers with acceptable voltage quality. The main contributions of this paper are summarized as follows.

- We propose a voltage-reactive power constrained HEMS optimization framework that can be carried out in three-phase unbalanced distribution systems. Unlike existing HEMS optimization methods that focuses on only the consumer energy savings under the TOU pricing tariff, the proposed framework minimizes the electricity cost in consumers' comfort level and improves the voltage quality for the consumer simultaneously. In the proposed framework, both the active and reactive power consumptions of unbalanced voltage-dependent loads together with the operation of the OLTC and smart inverters of the DERs are scheduled to achieve energy savings and maintain voltage quality.
- We formulate the proposed HEMS optimization algorithm as a MILP model. The models for three-phase unbalanced active/reactive power flow, voltage-dependent load, and OLTC are linearized and these linearized equations are incorporated as the constraints of the proposed MILP HEMS optimization problem. In a simulation, we compare the performance of the proposed HEMS to that of conventional HEMS in terms of active/reactive power consumption, three-phase voltage magnitudes, and the total cost of electricity. Simulation results confirm that the proposed HEMS can achieve more energy savings than a conventional HEMS. Further, we quantify the impact of voltage minimization on the proposed HEMS and verify that it could lead to a more significant reduction in reactive energy than in active energy.

The remainder of this paper is organized as follows. In Section II, we introduce the system model configuration and formulate the conventional HEMS optimization algorithm using MILP in the TOU pricing tariff, where the electricity price varies based on a different time block. The proposed voltage-reactive power constrained HEMS problem is formulated as an MILP problem in Section III. We then present the simulation results and discussions in Section IV and conclude the paper in Section V.

II. PRELIMINARIES

A. SYSTEM CONFIGURATION

We consider a radial LV distribution network that includes a medium-voltage (MV)/LV transformer with OLTC and multiple smart households along the distribution feeder as indicated in Fig. 1. The distribution feeder consists of a set of nodes $\mathcal{U}$ and a set of branches $\mathcal{L}$ (for example, $\mathcal{U} := \{0, 1, 2, \ldots, n\}$ and $\mathcal{L} := \{0 \to 1, 1 \to 2, \ldots, n-1 \to n\}$). Let a node $u \in \mathcal{U}$ and each line is formed by a pair of nodes $(u, v) \in \mathcal{L}$. We assume that a smart household is connected to each node u and is equipped with a PV system, an ESS, and smart household appliances. Multiple households that are supplied by the same LV system can form an entity, which is regarded as a community. In the residential community, we consider the situation in which each consumer

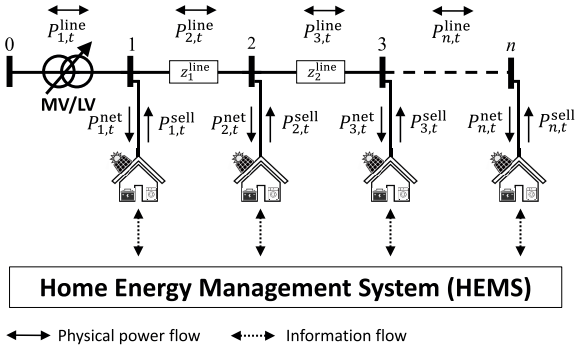

FIGURE 1. System model for home energy management in a LV distribution feeder.

(household) can exchange energy with the grid based on the TOU pricing scheme. Under the TOU pricing, consumers can reduce their electricity costs by scheduling their household appliances and injecting power to the grid while system operator reduces an aggregated power demand from consumers in order to reduce the system operational cost. We assume that a distribution system operator can collect power consumption data from consumers in the community. Therefore, the collected data is used by the community HEMS as input data to schedule the optimal energy consumption of households. In this paper, the main function of the community HEMS is to schedule the optimal energy consumption of appliances and power exchange of consumers while maintaining the consumer comfort and voltage level within their preferred and acceptable ranges.

The smart household appliances are classified into two types of loads: (1) uncontrollable load (e.g., TV, PC, and lighting); and (2) controllable load (e.g., air conditioner, washing machine, and ESS). Only the controllable load can be scheduled and operated by the HEMS. In this paper, an air conditioner is selected as the controllable load. We assume that both loads consume both active and reactive power and the reactive power consumption of loads are expressed in term of their real power consumption and power factor. We assume that PV system and ESS of each household have an individual smart inverter which has capability to regulate the voltage through injecting active power or injecting/absorbing reactive power in the system. In the considered LV system, voltage regulating devices are the OLTC transformer and smart inverters of PV system and ESS of each household.

B. CONVENTIONAL HEMS OPTIMIZATION MODEL

For each consumer (or household) $u \in \mathcal{U}$ with scheduling period $t \in \mathcal{T} := \{1, \ldots, T\}$ where $\mathcal{T}$ is the set of scheduling horizon, a general HEMS optimization problem is formulated as follows:

$$\min \underbrace{\sum_{u\in\mathcal{U}}\sum_{t\in\mathcal{T}}\left(\pi_t^{\text{buy}}P_{u,t}^{\text{net}} - \pi_t^{\text{sell}}P_{u,t}^{\text{sell}}\right)}_{J_1\left(P_{u,t}^{\text{net}}, P_{u,t}^{\text{sell}}\right)} + \underbrace{\sum_{u\in\mathcal{U}}\epsilon_u\sum_{t\in\mathcal{T}}\delta_{u,t}}_{J_2(\delta_{u,t})} \quad (1)$$

$$s.t.\ P^{\text{net}}_{u,t} = P^{\text{load}}_{u,t} + P^{\text{ESS,ch}}_{u,t} - P^{\text{PV,home}}_{u,t} - P^{\text{ESS,home,dch}}_{u,t} \quad (2)$$

$$P^{\text{sell}}_{u,t} = P^{\text{ESS,sell,dch}}_{u,t} + P^{\text{PV,sell}}_{u,t} \quad (3)$$

$$\widehat{P}^{\text{PV}}_{u,t} = P^{\text{PV,home}}_{u,t} + P^{\text{PV,sell}}_{u,t} \quad (4)$$

$$P^{\text{ESS,dch}}_{u,t} = P^{\text{ESS,home,dch}}_{u,t} + P^{\text{ESS,sell,dch}}_{u,t} \quad (5)$$

$$P^{\text{line}}_{uv,t} = \sum_{w \in \mathcal{D}_v} P^{\text{line}}_{vw,t} - P^{\text{node}}_{v,t}, \quad uv \in \mathcal{L} \quad (6)$$

$$P^{\text{node}}_{u,t} = P^{\text{net}}_{u,t} - P^{\text{sell}}_{u,t} \quad (7)$$

$$P^{\text{load}}_{u,t} = P^{\text{c}}_{u,t} + P^{\text{uc}}_{u,t} \quad (8)$$

$$SOC_{u,t} = SOC_{u,t-1} + \frac{\eta^{\text{ch}}_u P^{\text{ESS,ch}}_{u,t}}{E^{\text{ESS,max}}_u} - \frac{P^{\text{ESS,dch}}_{u,t}}{\eta^{\text{dch}}_u E^{\text{ESS,max}}_u} \quad (9)$$

$$T^{\text{in}}_{u,t} = T^{\text{in}}_{u,t-1} + \alpha_u(\widehat{T}^{\text{out}}_{u,t} - T^{\text{in}}_{u,t-1}) + \beta_u P^{\text{c}}_{u,t} \quad (10)$$

$$0 \le P^{\text{net}}_{u,t} \le N \cdot b^{\text{net}}_{u,t} \quad (11)$$

$$0 \le P^{\text{sell}}_{u,t} \le N \cdot (1 - b^{\text{net}}_{u,t}) \quad (12)$$

$$SOC^{\text{min}}_u \le SOC_{u,t} \le SOC^{\text{max}}_u \quad (13)$$

$$P^{\text{ESS,ch,min}}_u b^{\text{ESS}}_{u,t} \le P^{\text{ESS,ch}}_{u,t} \le P^{\text{ESS,ch,max}}_u b^{\text{ESS}}_{u,t} \quad (14)$$

$$P^{\text{ESS,dch,min}}_u (1 - b^{\text{ESS}}_{u,t}) \le P^{\text{ESS,dch}}_{u,t} \le P^{\text{ESS,dch,max}}_u (1 - b^{\text{ESS}}_{u,t}) \quad (15)$$

$$T^{\text{min}}_u - \delta_{u,t} \le T^{\text{in}}_{u,t} \le T^{\text{max}}_u + \delta_{u,t} \quad (16)$$

$$0 \le \delta_{u,t} \le \delta^{\text{max}}_u \quad (17)$$

$$P^{\text{c,min}}_u \le P^{\text{c}}_{u,t} \le P^{\text{c,max}}_u. \quad (18)$$

The objective function (1) for the HEMS optimization problem consists of two parts. The first part denotes the total electricity cost during the scheduling time period T. T is set to 24 hours with a one hour scheduling resolution. The total electricity cost is the difference between the electricity buying cost and electricity selling cost, corresponding to the net power consumption in household ($P^{\text{net}}_{u,t}$) with TOU-based buying price (π^{buy}_t) and net power supply ($P^{\text{sell}}_{u,t}$) with TOU-based selling price (π^{sell}_t). The second part J_2 represents the total amount of penalty ($\delta_{u,t}$), which involves the consumers' discomfort cost. Discomfort is the deviation of the consumers' preferred temperature from the indoor temperature. $\delta_{u,t}$ is a relaxation variable to guarantee the feasibility of the HEMS optimization problem. ϵ_u implies a penalty for $\delta_{u,t}$. For example, as ϵ_u increases, $\delta_{u,t}$ decreases, consequently ensuring the minimum deviation of the consumer's preferred temperature from the indoor temperature, however achieving less electricity cost saving. On the other hand, a decreasing ϵ_u yields an increasing $\delta_{u,t}$, which means that consumer's discomfort is larger, but with more electricity cost saving. In this paper, we assume that the value of this penalty coefficient is chosen by community HEMS operator based on each consumer preference.

Equation (2) illustrates the net energy consumption, i.e., the difference between the total active power consumption from all appliances ($P^{\text{load}}_{u,t}$) with the charging of the ESS ($P^{\text{ESS,ch}}_{u,t}$) and total active power supply from the PV system ($P^{\text{PV,home}}_{u,t}$) with the discharging of the ESS ($P^{\text{ESS,home,dch}}_{u,t}$) to a household. Equation (3) is the constraint on the consumer's selling power ($P^{\text{sell}}_{u,t}$) and consists of the discharging active power ($P^{\text{ESS,sell,dch}}_{u,t}$) of the ESS and injected active power ($P^{\text{PV,sell}}_{u,t}$) of the PV system. The predicted PV generation of the active power ($\widehat{P}^{\text{PV}}_{u,t}$) addresses the power consumption ($P^{\text{PV,home}}_{u,t}$) for the household and sells power ($PV^{\text{PV,sell}}_{u,t}$) to the grid in (4). Equation (5) implies that a total ESS discharging power ($P^{\text{ESS,dch}}_{u,t}$) supports power consumption ($P^{\text{ESS,home,dch}}_{u,t}$) in the household and sells power ($P^{\text{ESS,sell,dch}}_{u,t}$) to the grid. The balance equation for the active power flow is illustrated in (6) where the active power flow at branch uv ($P^{\text{line}}_{uv,t}$) is written in terms of the nodal active power ($P^{\text{node}}_{v,t}$) at consumer v and the sum of the active power flow from node v to node w where w is in a set of downstream nodes $\mathcal{D}_v$ that are connected to node v. The nodal active power $P^{\text{node}}_{u,t}$ is expressed as the gap between the net power consumption and net power supply to the grid in (7). Equation (8) illustrates that the active power load consumption $P^{\text{load}}_{u,t}$ is the sum of active power consumption for controllable load ($P^{c}_{u,t}$) (air conditioner in this paper) and uncontrollable load ($P^{uc}_{u,t}$). Equation (9) defines the operation of the state of charge (SOC) for the ESS at the current time t in terms of the SOC at the previous time t-1, battery capacity $E^{\text{ESS,max}}_u$, charging and discharging efficiency, η^{ch}_u and η^{dch}_u, respectively, and charging and discharging power for consumer u, $P^{\text{ESS,ch}}_{u,t}$ and $P^{\text{ESS,dch}}_{u,t}$, respectively. Equation (10) is the constraint for the temperature dynamics of the air conditioner at time t ($T^{\text{in}}_{u,t}$), which is expressed in terms of $T^{\text{in}}_{u,t-1}$ at time $t-1$, the predicted outdoor temperature at time t ($\widehat{T}^{\text{out}}_{u,t}$), power consumption of the air conditioner ($P^{\text{c}}_{u,t}$), and the environmental parameters (α_u, β_u) that specify the indoor thermal condition. Equations (11) and (12) ensure that the buying and selling of power from/to the grid do not occur simultaneously. Equation (13) provides the capacity constraint of the SOC for the ESS. Equations (14) and (15) present the constraints on the charging ($P^{\text{ESS,ch}}_{u,t}$) and discharging power ($P^{\text{ESS,dch}}_{u,t}$) of the ESS, respectively, where $b^{\text{ESS}}_{u,t}$ represents the binary decision variable that determines the charging/discharging status of the ESS. Equation (16) presents the range of the relaxed indoor temperature. The relaxation variable $\delta_{u,t}$ in (16) is limited by δ^{max}_u in (17). The capacity of the power consumption of the air conditioner is described in (18).

We note that the aforementioned conventional HEMS approach neglects the actual distribution system parameters, network topology, and operating conditions such as: i) line impedance (z^{line}), ii) unbalanced distribution feeder and voltage-dependent load models, iii) reactive power consumption of home appliance, and iv) voltage regulation with the DERs and OLTC. The aforementioned limitations are addressed in the proposed HEMS optimization problem, which is illustrated in the following section.

III. PROPOSED HOME ENERGY MANAGEMENT OPTIMIZATION FRAMEWORK

In this section, we propose an optimization algorithm to schedule the energy consumption of household appliances

and power trades in multiple smart households considering voltage control and the reactive power dispatch of DERs. The proposed algorithm is implemented in a three-phase unbalanced distribution network (phase $\phi \in \Phi := \{a, b, c\}$) with the same network topology as Fig. 1. The proposed HEMS algorithm with the constraints of the conventional HEMS (2)–(7), (9)–(18) can be formulated as follows.

$$\min \underbrace{\sum_{u\in\mathcal{U}}\sum_{\phi\in\Phi}\sum_{t\in\mathcal{T}}\left(\pi_t^{\text{buy}}P_{u,\phi,t}^{\text{net}} - \pi_t^{\text{sell}}P_{u,\phi,t}^{\text{sell}}\right)}_{J_1\left(P_{u,\phi,t}^{\text{net}}, P_{u,\phi,t}^{\text{sell}}\right)} + \underbrace{\sum_{u\in\mathcal{U}}\sum_{\phi\in\Phi}\epsilon_{u,\phi}\sum_{t\in\mathcal{T}}\delta_{u,\phi,t}}_{J_2\left(\delta_{u,\phi,t}\right)}$$

$$s.t.\begin{cases}\text{Reactive power constraints : Eqn. (20) – (22)}\\ \text{Three-phase linear voltage constraint : Eqn. (23)}\\ \text{Voltage-dependent load models : Eqn. (29) – (38)}\\ \text{Reactive power of PV and ESS : Eqn. (39) – (40)}\\ \text{Voltage and OLTC tap change : Eqn. (41) – (43)}\end{cases} \tag{19}$$

A. REACTIVE POWER CONSTRAINTS

Equation (20) expresses the nodal net reactive power consumption ($Q_{u,\phi,t}^{\text{node}}$) of consumer u for phase ϕ at time t in terms of reactive load power consumption ($Q_{u,\phi,t}^{\text{load}}$) and injected or absorbed reactive power from PV ($Q_{u,\phi,t}^{\text{PV}}$) and ESS ($Q_{u,\phi,t}^{\text{ESS}}$). The balance equation of the reactive power flow is illustrated in (21), where the reactive power flow at branch uv ($Q_{uv,\phi,t}^{\text{line}}$) is written in terms of the nodal reactive power ($Q_{v,\phi,t}^{\text{node}}$) at consumer v and the sum of the reactive power flow from node v to node w where w is in a set of downstream nodes $\mathcal{D}_v$ that are connected to node v. The reactive power consumption of the air conditioner is described in terms of its power factor ($\text{PF}_{u,\phi}$) and active power consumption ($P_{u,\phi,t}^{\text{c}}$).

$$Q_{u,\phi,t}^{\text{node}} = Q_{u,\phi,t}^{\text{load}} - Q_{u,\phi,t}^{\text{PV}} - Q_{u,\phi,t}^{\text{ESS}} \tag{20}$$

$$Q_{uv,\phi,t}^{\text{line}} = \sum_{w\in\mathcal{D}_v} Q_{vw,\phi,t}^{\text{line}} - Q_{v,\phi,t}^{\text{node}}, \quad uv \in \mathcal{L} \tag{21}$$

$$Q_{u,\phi,t}^{\text{c}} = \sqrt{\frac{1-\text{PF}_{u,\phi}^2}{\text{PF}_{u,\phi}^2}}P_{u,\phi,t}^{\text{c}}. \tag{22}$$

B. LINEAR THREE-PHASE UNBALANCED POWER FLOW CONSTRAINTS

We denote the complex vector and matrix of the voltage, current, and line impedance by $\mathbf{V}_u, \mathbf{I}_{uv}^{\text{line}} \in \mathbb{C}^{3\times 1}$, and $\mathbf{z}_{uv}^{\text{line}} \in \mathbb{C}^{3\times 3}$. Using the linearization method introduced from [34] with Kirchhoff's voltage law $\mathbf{V}_v = \mathbf{V}_u - \mathbf{z}_{uv}^{\text{line}}\mathbf{I}_{uv}^{\text{line}}$, the relationship of voltage between consumers u and v can be written as

$$\mathbf{V}_{v,t}^{\text{sq}} = \mathbf{V}_{u,t}^{\text{sq}} - \tilde{\mathbf{z}}_{uv}^{\text{line}}(\mathbf{P}_{uv,t}^{\text{line}} + j\mathbf{Q}_{uv,t}^{\text{line}})^* - (\tilde{\mathbf{z}}_{uv}^{\text{line}})^*(\mathbf{P}_{uv,t}^{\text{line}} + j\mathbf{Q}_{uv,t}^{\text{line}}) \tag{23}$$

where $\mathbf{V}_{u,t}^{\text{sq}} \in \mathbb{R}^{3\times 1}$ is the vector of the square of the three-phase voltage magnitude for consumer u at time t, $\mathbf{P}_{uv,t}^{\text{line}} = [\mathbf{P}_{uv,a,t}^{\text{line}}, \mathbf{P}_{uv,b,t}^{\text{line}}, \mathbf{P}_{uv,c,t}^{\text{line}}]^T$ and $\mathbf{Q}_{uv,t}^{\text{line}} = [\mathbf{Q}_{uv,a,t}^{\text{line}}, \mathbf{Q}_{uv,b,t}^{\text{line}}, \mathbf{Q}_{uv,c,t}^{\text{line}}]^T$ are the three-phase active and reactive line flow of line uv at time t, respectively, and $\tilde{\mathbf{z}}_{uv}^{\text{line}} = \gamma \otimes \mathbf{z}_{uv}^{\text{line}}$. Here, the symbol $\otimes$ represents elementwise multiplication, and γ is defined as

$$\boldsymbol{\gamma} = \begin{bmatrix} 1 & e^{-j2\pi/3} & e^{j2\pi/3} \\ e^{j2\pi/3} & 1 & e^{-j2\pi/3} \\ e^{-j2\pi/3} & e^{j2\pi/3} & 1 \end{bmatrix}. \tag{24}$$

C. VOLTAGE-DEPENDENT LOAD MODEL CONSTRAINTS

In order to incorporate the relationship between load consumption and voltage magnitude in the optimization problem, ZIP load models for both active and reactive powers are adopted. Active and reactive powers of load for each phase of node u at time t are modeled as

$$\frac{P_{u,\phi,t}^{\text{load}}}{P_{u,\phi,t}^{\text{load,nom}}} = c_p^Z\left(\frac{V_{u,\phi,t}}{V^{\text{nom}}}\right)^2 + c_p^I\frac{V_{u,\phi,t}}{V^{\text{nom}}} + c_p^P \tag{25}$$

$$\frac{Q_{u,\phi,t}^{\text{load}}}{Q_{u,\phi,t}^{\text{load,nom}}} = c_q^Z\left(\frac{V_{u,\phi,t}}{V^{\text{nom}}}\right)^2 + c_q^I\frac{V_{u,\phi,t}}{V^{\text{nom}}} + c_q^P. \tag{26}$$

Here, $P(Q)_{u,\phi,t}^{\text{load,nom}}$ are active(reactive) power consumption of load at nominal voltage V^{nom}, $\{c_p^Z, c_p^I, c_p^P\}$ and $\{c_q^Z, c_q^I, c_q^P\}$ are the sets of the coefficients that illustrate the percentage of constant impedance, constant current and constant power loads for active and reactive powers, respectively, with $c_p^Z + c_p^I + c_p^P = 1$ and $c_q^Z + c_q^I + c_q^P = 1$. Then, let the equations (25) and (26) be rewritten in term of square of voltage magnitude ($V_{u,\phi,t}^{\text{sq}}$) instead of voltage magnitude ($V_{u,\phi,t}$) as shown below

$$\frac{P_{u,\phi,t}^{\text{load}}}{P_{u,\phi,t}^{\text{load,nom}}} = c_p^Z\frac{V_{u,\phi,t}^{\text{sq}}}{(V^{\text{nom}})^2} + c_p^I\frac{\sqrt{V_{u,\phi,t}^{\text{sq}}}}{V^{\text{nom}}} + c_p^P \tag{27}$$

$$\frac{Q_{u,\phi,t}^{\text{load}}}{Q_{u,\phi,t}^{\text{load,nom}}} = c_q^Z\frac{V_{u,\phi,t}^{\text{sq}}}{(V^{\text{nom}})^2} + c_q^I\frac{\sqrt{V_{u,\phi,t}^{\text{sq}}}}{V^{\text{nom}}} + c_q^P. \tag{28}$$

Based on [34], the nonlinear term $\sqrt{V_{u,\phi,t}^{\text{sq}}}$ in (27) and (28) can be linearized as $\sqrt{V_{u,\phi,t}^{\text{sq}}} \approx 0.5 + 0.5V_{u,\phi,t}^{\text{sq}}$. Finally, the linearized ZIP models of the three-phase active and reactive loads for consumer u at time t are described as

$$\mathbf{P}_{u,t}^{\text{load}} = \boldsymbol{\omega}_{u,t}^P\left(\frac{c_p^Z}{(V^{\text{nom}})^2} + 0.5\frac{c_p^I}{V^{\text{nom}}}\right) + \mathbf{P}_{u,t}^{\text{load,nom}}\left(0.5\frac{c_p^I}{V^{\text{nom}}} + c_p^P\right) \tag{29}$$

$$\mathbf{Q}_{u,t}^{\text{load}} = \boldsymbol{\omega}_{u,t}^Q\left(\frac{c_q^Z}{(V^{\text{nom}})^2} + 0.5\frac{c_q^I}{V^{\text{nom}}}\right) + \mathbf{Q}_{u,t}^{\text{load,nom}}\left(0.5\frac{c_q^I}{V^{\text{nom}}} + c_q^P\right). \tag{30}$$

Here, for $\boldsymbol{\omega}_{u,t}^{P(Q)} \in \mathbb{R}_{\geq 0}^{3\times 1}$ and $\mathbf{P(Q)}_{u,t}^{\text{load,nom}} \in \mathbb{R}_{\geq 0}^{3\times 1}$, $\boldsymbol{\omega}_{u,t}^{P(Q)}$ are defined as $\mathbf{P(Q)}_{u,t}^{\text{load,nom}} \otimes \mathbf{V}_{u,t}^{\text{sq}}$. The two additional variable vectors $\boldsymbol{\omega}_{u,t}^{P(Q)}$ are introduced based on the McCormick Envelopes relaxation technique [35] and are bounded by

$$\boldsymbol{\omega}_{u,t}^{P(Q)} \geq \mathbf{P(Q)}^{\text{load,nom,min}} \otimes \mathbf{V}_{u,t}^{\text{sq}} + \mathbf{P(Q)}_{u,t}^{\text{load,nom}} \otimes \mathbf{V}^{\text{min,sq}} - \mathbf{P(Q)}^{\text{load,nom,min}} \otimes \mathbf{V}^{\text{min,sq}} \quad (31)$$

$$\boldsymbol{\omega}_{u,t}^{P(Q)} \geq \mathbf{P(Q)}^{\text{load,nom,max}} \otimes \mathbf{V}_{u,t}^{\text{sq}} + \mathbf{P(Q)}_{u,t}^{\text{load,nom}} \otimes \mathbf{V}^{\text{max,sq}} - \mathbf{P(Q)}^{\text{load,nom,max}} \otimes \mathbf{V}^{\text{max,sq}} \quad (32)$$

$$\boldsymbol{\omega}_{u,t}^{P(Q)} \leq \mathbf{P(Q)}^{\text{load,nom,max}} \otimes \mathbf{V}_{u,t}^{\text{sq}} + \mathbf{P(Q)}_{u,t}^{\text{load,nom}} \otimes \mathbf{V}^{\text{min,sq}} - \mathbf{P(Q)}^{\text{load,nom,max}} \otimes \mathbf{V}^{\text{min,sq}} \quad (33)$$

$$\boldsymbol{\omega}_{u,t}^{P(Q)} \leq \mathbf{P(Q)}^{\text{load,nom,min}} \otimes \mathbf{V}_{u,t}^{\text{sq}} + \mathbf{P(Q)}_{u,t}^{\text{load,nom}} \otimes \mathbf{V}^{\text{max,sq}} - \mathbf{P(Q)}^{\text{load,nom,min}} \otimes \mathbf{V}^{\text{max,sq}}. \quad (34)$$

Equations (31), (32) and (33), (34) are underestimators and overestimators of the two additional variable vectors, respectively. These bounds are derived from the assumption that bounds of variables $\mathbf{P(Q)}_{u,t}^{\text{load,nom}}$ and $\mathbf{V}_{u,t}^{\text{sq}}$ are known.

Equations (35) and (36) display the limit of the nominal active and reactive power consumption of loads.

$$\mathbf{P}^{\text{load,nom,min}} \leq \mathbf{P}_{u,t}^{\text{load,nom}} \leq \mathbf{P}^{\text{load,nom,max}} \quad (35)$$

$$\mathbf{Q}^{\text{load,nom,min}} \leq \mathbf{Q}_{u,t}^{\text{load,nom}} \leq \mathbf{Q}^{\text{load,nom,max}}. \quad (36)$$

The three-phase active and reactive load consumptions at nominal voltage for consumer u at time t are expressed in terms of the active and reactive power consumption of the controllable ($\mathbf{P}_{u,t}^{\text{c}}, \mathbf{Q}_{u,t}^{\text{c}} \in \mathbb{R}_{\geq 0}^{3\times 1}$) and uncontrollable appliances ($\mathbf{P}_{u,t}^{\text{uc}}, \mathbf{Q}_{u,t}^{\text{uc}} \in \mathbb{R}_{\geq 0}^{3\times 1}$) as follows:

$$\mathbf{P}_{u,t}^{\text{load,nom}} = \mathbf{P}_{u,t}^{\text{c}} + \mathbf{P}_{u,t}^{\text{uc}} \quad (37)$$

$$\mathbf{Q}_{u,t}^{\text{load,nom}} = \mathbf{Q}_{u,t}^{\text{c}} + \mathbf{Q}_{u,t}^{\text{uc}}. \quad (38)$$

D. CONSTRAINTS FOR REACTIVE POWER OF PV AND ESS

Equations (39) and (40) show the capacity limits of the reactive power supported by the PV system and ESS.

$$Q_{u,\phi}^{\text{PV,min}} \leq Q_{u,\phi,t}^{\text{PV}} \leq Q_{u,\phi}^{\text{PV,max}} \quad (39)$$

$$Q_{u,\phi}^{\text{ESS,min}} \leq Q_{u,\phi,t}^{\text{ESS}} \leq Q_{u,\phi}^{\text{ESS,max}}. \quad (40)$$

E. CONSTRAINTS FOR VOLTAGE AND OLTC OPERATION

Equation (41) limits the range of the square voltage magnitude for consumer u with the minimum ($\mathbf{V}^{\text{min,sq}}$) and maximum ($\mathbf{V}^{\text{max,sq}}$) allowed value

$$\mathbf{V}^{\text{min,sq}} \leq \mathbf{V}_{u,t}^{\text{sq}} \leq \mathbf{V}^{\text{max,sq}}. \quad (41)$$

Equation (42) represents the square of the reference node voltage magnitude, which can be computed by the multiplication of the square nominal voltage magnitude $\mathbf{V}^{\text{nom,sq}}$ and the square of OLTC turn ratio, $\mathbf{a}_t^{\text{OLTC,sq}} = \left[a_{a,t}^{\text{OLTC,sq}}, a_{b,t}^{\text{OLTC,sq}}, a_{c,t}^{\text{OLTC,sq}}\right]^T$ that is determined by the OLTC tap position.

$$\mathbf{V}_{1,t}^{\text{sq}} = \mathbf{a}_t^{\text{OLTC,sq}} \otimes \mathbf{V}^{\text{nom,sq}}. \quad (42)$$

In (42), the square of OLTC turn ratio $a_{\phi,t}^{\text{OLTC,sq}}$ is derived as follows. Let $a_{\phi,t}^{\text{OLTC}} = \sum_{i\in\mathcal{N}^{\text{Tap}}} r_i U_{\phi,t,i}^{\text{Tap}}$ derived from [8]. Here, r_i is an element in a set of turn ratio of OLTC $\mathcal{R} = \{0.9, 0.90625, \ldots, 1.1\}$, $\mathcal{N}^{\text{Tap}}$ is a set of tap positions corresponding to turn ratio of OLTC, and $U_{\phi,t,i}^{\text{Tap}} \in \{0, 1\}$ is used to determine a proper turn ratio in the set. The OLTC is assumed to regulate voltage with a range of $\pm 10\%$ from nominal voltage, and each tap position changes with 0.00625 p.u. turn ratio step size. Let $(r_i)^2 = R_i$ and binary variable $\left(U_{\phi,t,i}^{\text{Tap}}\right)^2 = U_{\phi,t,i}^{\text{Tap}}$. Then, the square of OLTC turn ratio can be expressed as

$$a_{\phi,t}^{\text{OLTC,sq}} = \sum_{i\in\mathcal{N}^{\text{Tap}}} R_i U_{\phi,t,i}^{\text{Tap}}. \quad (43)$$

IV. NUMERICAL EXAMPLES

In this section, we analyze the performance of the proposed HEMS algorithm in the modified LV CIGRE distribution network [36] as shown in Fig. 2. Section IV-A provides the simulation setup for the proposed HEMS. The performance of the proposed approach is analyzed and evaluated in Section IV-B. In Section IV-B, the performance of the proposed HEMS (Section III) is first evaluated and validated in terms of the voltage level of the distribution feeder and scheduled active/reactive power. Then, the performance between the conventional HEMS (Section II-B) and the proposed HEMS is compared in terms of active power consumption and electricity cost. Finally, the impact of additional objective and constraints that minimize the feeder voltage magnitude on the proposed HEMS is investigated..

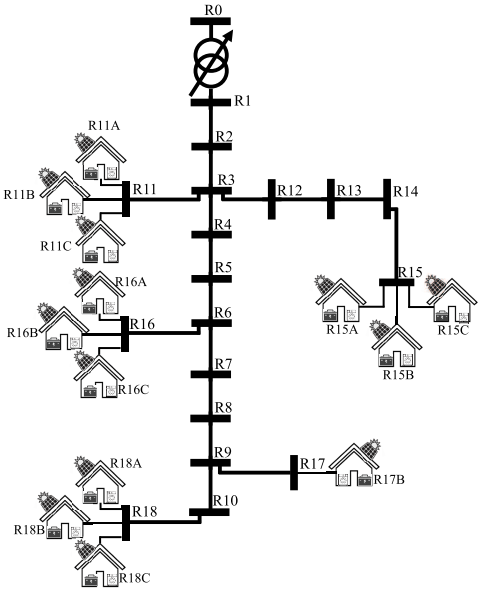

FIGURE 2. Modified CIGRE low voltage distribution network with OLTC and smart households equipped with home appliances, PV systems, and ESSs.

A. SIMULATION SETUP

As indicated in Fig. 2, smart households are connected to five nodes (R11, R15∼R18) from 18 nodes with different

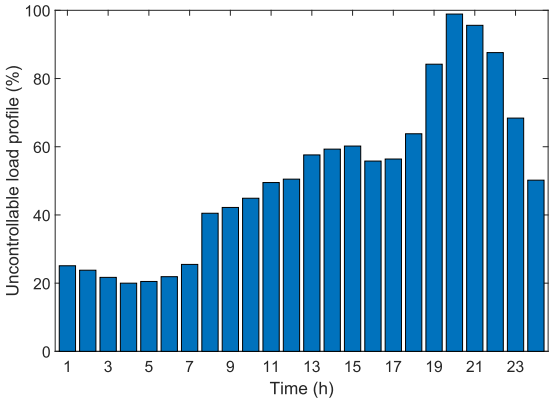

FIGURE 3. Predicted uncontrollable household load profile.

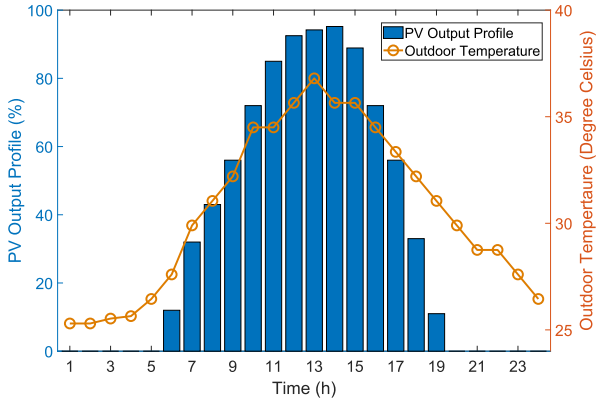

FIGURE 4. Profiles of predicted PV generation active power and outdoor temperature.

types of connections: a three-phase load for nodes R11, R15, R16, and R18, and single-phase load for node R17. We assume that each smart household has different nominal load consumption which consists of both controllable load (e.g., air conditioner) and uncontrollable load (e.g., TV, lighting, refrigerator, cooking appliances), where the consumption profile of the uncontrollable load is identical among the smart households as shown in Fig. 3. The OLTC at reference node R0 has a $\pm 10\%$ regulator range from the nominal voltage with 0.00625 p.u. step size, and the turn ratio r_i belongs to the set $\mathcal{R} = \{0.9, 0.90625, \ldots, 1.1\}$. The voltage magnitudes at all nodes in the system are limited in the range of [0.95, 1.05] p.u., which means that the square of voltage magnitudes are bounded in $[0.95^2, 1.05^2]$ p.u.. The sizes of the PV system and ESS connected to each household, are 3.25 kW and 0.5 kW, respectively, with a battery capacity of $E_u^{\mathrm{ESS,max}} = 2$ kWh. The PV generation active power output is assumed identical among all households as shown in Fig. 4. For the ESSs, the maximum charging/discharging power is 0.5 kW, and the minimum charging/discharging power is 0 kW. The initial, minimum, and maximum SOCs are 50%, 25%, and 100%, respectively. The charging (η_u^{ch}) and discharging (η_u^{dch}) efficiencies are both 95%. For each household, the comfortable temperature range prior to relaxation is assumed

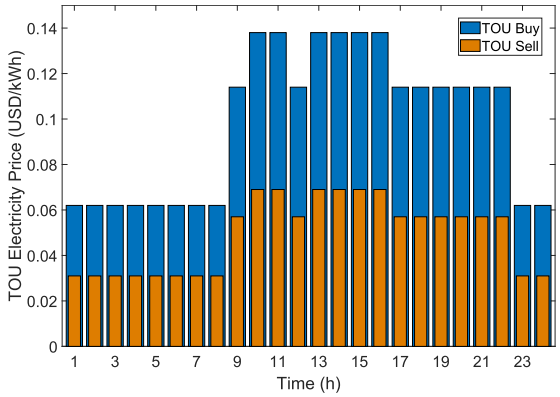

FIGURE 5. Profile of TOU price.

to be [22°C,24°C] with the maximum relaxed temperature $\delta_u^{\max} = 2$°C. Parameters α and β in the dynamic indoor temperature constraint are set to 0.9 and -0.0095, respectively. The maximum power consumption ($P_u^{\mathrm{c,max}}$) of the air conditioner is 1.14 kW. The outdoor temperature profile and TOU tariffs for the purchase price of the electricity are shown in Fig. 4 and Fig. 5, respectively, which are obtained from [28]. We assume that the selling price of the electricity is half of the purchase price in the TOU tariffs as shown in Fig. 5. The coefficients for the ZIP load models are provided in Table 1 [4]. The numerical testing was performed using the IBM ILOG CPLEX Optimization Studio 12.8 on an Intel Core i3-4160 with a 3.6 GHz CPU, 8 GB of RAM, and 64-bit operating system PC.

TABLE 1. ZIP Coefficients for Active and Reactive Load Model.

ZIP Coefficient	Active Load	Reactive Load
Z	1.5	7.41
I	-2.31	-11.97
P	1.81	5.55

B. PERFORMANCE ASSESSMENT OF THE PROPOSED HEMS

In this case, we first demonstrate the performance of the proposed HEMS in terms of the distribution feeder voltage level. Fig. 6 shows the values of the three-phase voltage magnitude for each node at 2 P.M. and 8 P.M., corresponding to two peak periods for PV generation output and load demand. We can observe from this figure that the voltage magnitudes at all the nodes are maintained within the lower half of the allowable voltage range [0.95 p.u., 1.05 p.u.]. This observation is because a lower voltage magnitude reduces power consumption of the voltage-dependent load and allows consumers to obtain more available power to be sold to the grid. This justification is consistent with the role of the first term of the multi-objective function (19) in the proposed HEMS. Another observation is that all the nodes at 2 P.M. have the minimum voltage magnitude values identically.

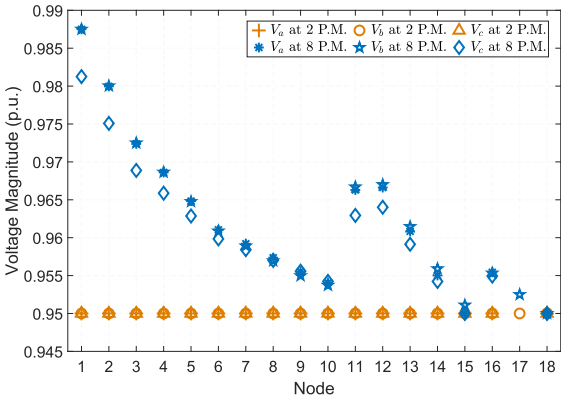

FIGURE 6. Three-phase voltage magnitudes in the test system at 2 P.M. and 8 P.M.

This derives from the fact that a high PV generation output at 2 P.M. increases the voltage level locally, which provides more room for the OLTC to reduce and flatten the entire feeder voltage level by reducing its tap position. Conversely, at the peak demand period of 8 P.M. without PV generation, the increase of the demand can result in a violation of the minimum voltage limit at certain nodes. To prevent this voltage violation, the OLTC attempts to raise its tap positions.

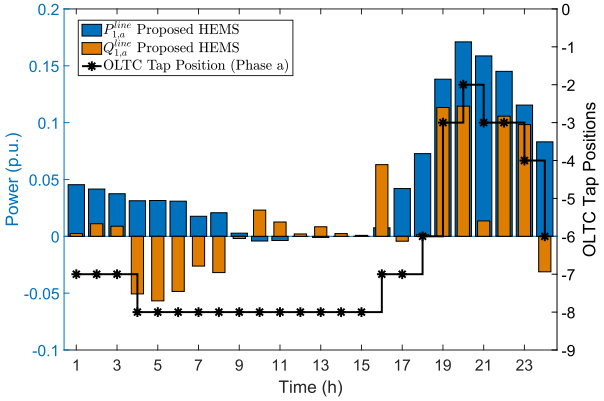

FIGURE 7. Total active/reactive power flow and OLTC tap position for phase *a*.

Figs. 7, 8 and 9 show the schedules of the total active/reactive power flow and the OLTC tap position for phases *a*, *b* and *c*, respectively. In these figures, the left and right *y*-axis correspond to the total active/reactive power flow and the OLTC tap position, respectively. We can observe from these figures that, throughout the day, the OLTC has a negative tap position for any phase. This observation justifies the results in Fig. 6, which show that the three-phase voltage magnitudes are below 1 p.u. due to a negative tap position of the OLTC. In Figs. 7, 8 and 9, the scheduled OLTC tap positions are categorized into four different scheduling intervals under varying load conditions and PV/ESS active/reactive power: i) the tap positions becomes lowered under light load condition (1∼3 A.M.); ii) the tap positions become the lowest due to mainly the reactive power injection from the smart

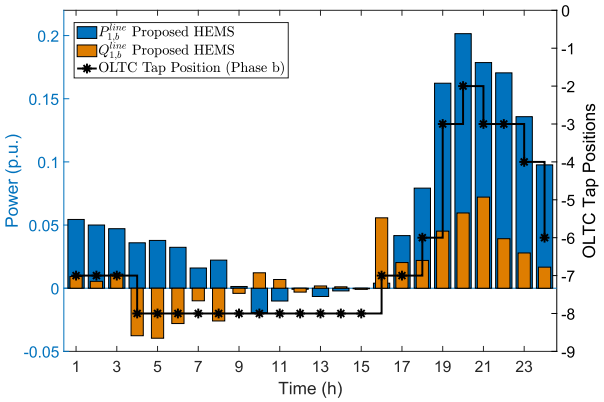

FIGURE 8. Total active/reactive power flow and OLTC tap position for phase *b*.

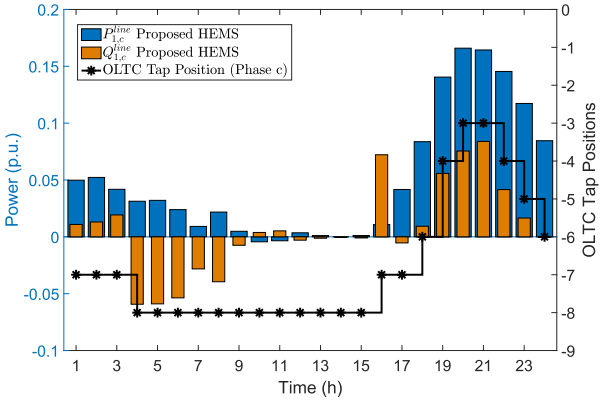

FIGURE 9. Total active/reactive power flow and OLTC tap position for phase *c*.

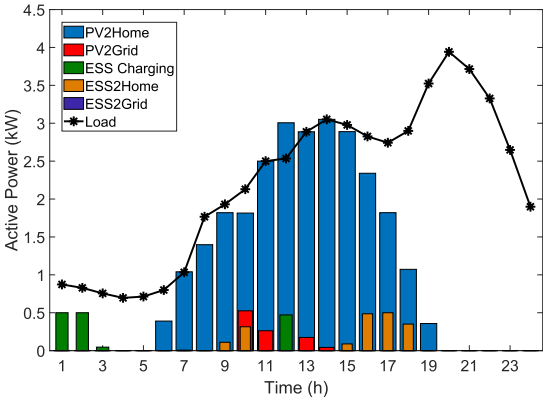

FIGURE 10. Active power consumption schedules in household R11B.

inverters of the PV system and ESS (4∼8 A.M.) and due to both the active and reactive power injection from the smart inverters of the PV system and ESS during PV generation period (9 A.M.∼3 P.M.); iii) the tap positions become higher under heavy load condition (4 P.M.∼8 P.M.); and iv) the tap positions become lowered (9 P.M.∼12 A.M.) because system loads become lighter after the peak load condition. We can verify from this observation that in the proposed

HEMS approach the optimal energy consumption schedules for smart households can be calculated through the coordination of the OLTC and smart inverters.

Fig. 10 shows the scheduled active power of household R11B at node R11 phase *b* for a 24-hour period. In this figure, the active power consumption is categorized into six types: 1) PV active power injecting to supply the household load (PV2Home), 2) PV active power injecting to the grid (PV2Grid), 3) ESS active power charging (ESS Charging), 4) ESS active power discharging to supply the household loads (ESS2Home), 5) ESS active power discharging to the grid (ESS2Grid), and 6) active power consumption of the controllable and uncontrollable loads (Load). We observe from Fig. 10 that during the PV generation period, the majority of the PV generation supports the household demand (PV2Home) including the controllable and uncontrollable loads, with a small amount of ESS charging power (ESS Charging) and selling power to the grid (PV2Grid). It should be noted that the ESS discharging power only addresses a portion of the household demand (ESS2Home) without being sold back to the grid (ESS2Grid). This implies that at any scheduling period, the selling price is not sufficiently high for a consumer to sell the ESS charging power to the grid to realize a profit. We also observe from this figure that in general, the ESS charging and discharging schedule relies on the TOU pricing tariffs and household load consumption profile. The ESS is charged during the scheduling periods with a low electricity price and low load demand period (1∼3 A.M. and 12 P.M.) whereas it is discharged during the scheduling periods with high electricity price and high load demand period (9∼10 A.M. and 3∼6 P.M.).

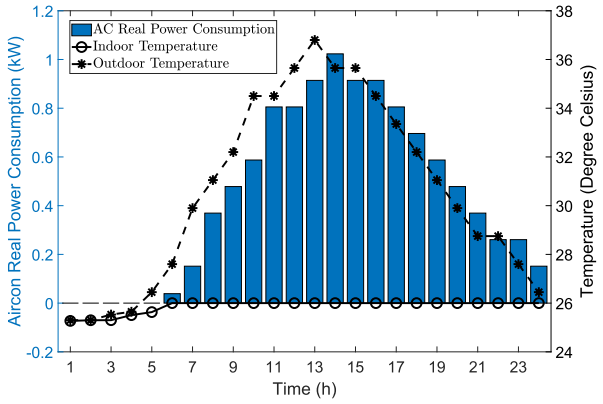

FIGURE 11. Schedules for active power consumption of air conditioner and indoor temperature in household R11B given outdoor temperature profile.

Fig. 11 shows active power consumption schedules for air conditioner along with the indoor and outdoor temperature of household R11B. In this figure, the left and right *y*-axis correspond to the active power consumption of air conditioner and the indoor/outdoor temperature, respectively. We can observe from Fig. 11 that as the outdoor temperature increases, the active power consumption of air conditioner also increases while maintaining the indoor temperature within the consumer preferred indoor temperature range. It is noted in this simulation study that the initial preferred indoor temperature range [22^{o}C, 24^{o}C] is relaxed with $\delta^{\max} = 2^o$C so that the indoor temperature increases to 26^{o}C (6 A.M.∼12 A.M.). This relaxation prevents the HEMS optimization problem from becoming infeasible and enables the HEMS to calculate the optimal energy consumption schedule for households.

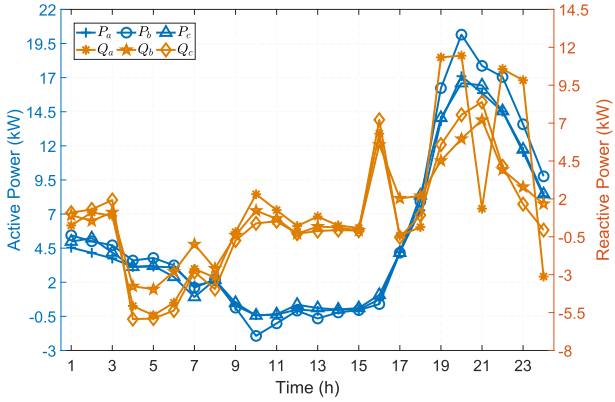

FIGURE 12. Aggregate three-phase active and reactive power consumption schedules in the proposed HEMS.

Fig. 12 illustrates the values of the three-phase active and reactive power injected from the OLTC transformer for a 24-hour period. We can observe from this figure that three-phase reactive power is unbalanced and fluctuating more than the three-phase active power. This is because to maintain the consumers' voltage quality and reduction of their electricity cost, the PV systems and ESSs frequently regulate the feeder voltage using the reactive power more than the active power during the total scheduling period.

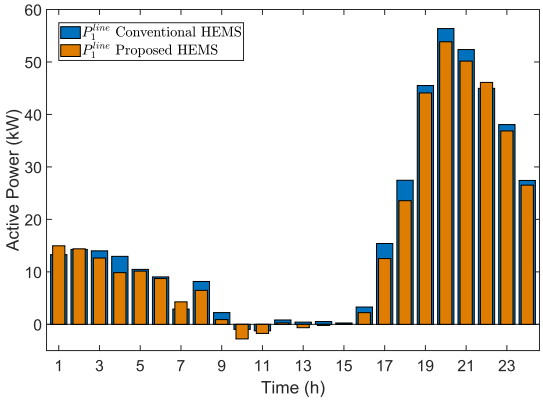

FIGURE 13. Comparison of total active power consumption schedules between the conventional HEMS and the proposed HEMS.

Next, we compare the performance of the conventional HEMS and proposed HEMS in terms of scheduled active power fed by transformer. For a fair comparison, both systems are tested in an environment where all operating parameters and conditions to schedule home energy are identical except for the proposed HEMS having the additional constraints associated with reactive power and voltage quality. Fig. 13 indicates that the active power consumption of the

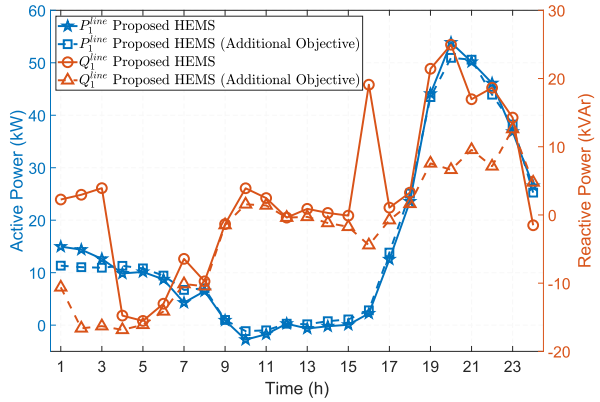

FIGURE 14. Comparison of total active/reactive power consumption schedules between the proposed HEMS without and with voltage minimization term.

proposed HEMS is marginally less than that of the conventional HEMS during the majority of the scheduling periods. This observation is natural because the proposed HEMS enables the OLTC, PV systems, and ESSs as voltage regulators to decrease the voltage level for reducing the active power consumption. However, this observation is not always true at certain scheduling periods, for example in the following situation. Whereas the ESS, through charging the active power, decreases the voltage for reducing the active power consumption of the load, the amount of the ESS charging power could be greater than the amount of the reduction of the load power consumption. In this situation, the active power consumption in the proposed HEMS would become greater than in the conventional HEMS.

Next, we investigate the impact of voltage minimization on the proposed HEMS. To this end, we reformulate the proposed HEMS optimization problem with additional objective function J_3 in (44) and constraints (45), (46) [37] as follows:

$$\min \underbrace{\sum_{u\in\mathcal{U}}\sum_{\phi\in\Phi}\sum_{t\in\mathcal{T}}\left(\pi_t^{\text{buy}}P_{u,\phi,t}^{\text{net}}-\pi_t^{\text{sell}}P_{u,\phi,t}^{\text{sell}}\right)}_{J_1\left(P_{u,\phi,t}^{\text{net}},P_{u,\phi,t}^{\text{sell}}\right)} + \underbrace{\sum_{u\in\mathcal{U}}\sum_{\phi\in\Phi}\epsilon_{u,\phi}\sum_{t\in\mathcal{T}}\delta_{u,\phi,t}}_{J_2(\delta_{u,\phi,t})} + \underbrace{\sum_{u\in\mathcal{U}}\sum_{\phi\in\Phi}\sum_{t\in\mathcal{T}}\lambda_{u,\phi,t}}_{J_3(\lambda_{u,\phi,t})} \quad (44)$$

and

$$\lambda_{u,\phi,t} = V_{u,\phi,t}^{\text{sq}} - V^{\min,\text{sq}} \quad (45)$$

$$\lambda_{u,\phi,t} \geq 0. \quad (46)$$

In (44), the newly added objective function $J_3\left(\lambda_{u,\phi,t}\right)$ represents the total gap between the square voltages and their lowest limits for all nodes and phases during the prediction horizon. The gap of the square voltage at each consumer is defined in (45); this voltage gap is ensured to be non-negative in (46). This objective function and the constraints are to decrease the voltage profile as close as to its minimum limit and hence, reduce the energy consumption while maintaining the voltage quality. Fig. 14 compares the scheduled active and reactive powers between the proposed HEMS algorithms with and without the voltage minimization. We first observe from this figure that the difference of the active powers between the two algorithms for a 24-hour period is reasonably small, and conclude that the voltage minimization has no significant impact on the active power scheduling. This small difference occurs because the voltage minimization influences both the charging and discharging process of the ESS for minimizing the voltage magnitude and increasing the electricity cost savings simultaneously. However, as indicated in Fig. 14, we observe that the HEMS algorithm with the voltage minimization yields a greater reduction of the reactive power than without the voltage minimization. This is because PV system and ESS of each household regulate voltage magnitude with their reactive power capability by injecting more reactive power than absorbing reactive power.

TABLE 2. Active/Reactive Power Consumption and Electricity Cost for thirteen households in the System during 24 hours.

Household	Description	HEMS 1	HEMS 2	HEMS 3
R11A	Active Energy (kWh)	33.36	31.49	31.47
	Reactive Energy (kVArh)	NA	20.63	5.20
	Electricity Cost (USD)	3.18	2.98	2.98
R11B	Active Energy (kWh)	26.95	25.28	25.31
	Reactive Energy (kVArh)	NA	33.55	15.21
	Electricity Cost (USD)	2.55	2.40	2.40
R11C	Active Energy (kWh)	30.61	28.29	28.80
	Reactive Energy (kVArh)	NA	26.22	4.43
	Electricity Cost (USD)	2.89	2.72	2.72
R15A	Active Energy (kWh)	30.61	28.66	28.67
	Reactive Energy (kVArh)	NA	12.55	5.62
	Electricity Cost (USD)	2.89	2.70	2.71
R15B	Active Energy (kWh)	28.78	26.90	26.94
	Reactive Energy (kVArh)	NA	-6.50	-14.00
	Electricity Cost (USD)	2.72	2.54	2.54
R15C	Active Energy (kWh)	32.44	30.43	30.53
	Reactive Energy (kVArh)	NA	-7.03	-13.85
	Electricity Cost (USD)	3.08	2.87	2.89
R16A	Active Energy (kWh)	28.78	26.95	26.99
	Reactive Energy (kVArh)	NA	5.00	-9.73
	Electricity Cost (USD)	2.72	2.55	2.55
R16B	Active Energy (kWh)	33.36	31.36	31.47
	Reactive Energy (kVArh)	NA	16.27	2.91
	Electricity Cost (USD)	3.18	2.97	2.98
R16C	Active Energy (kWh)	28.78	26.94	26.98
	Reactive Energy (kVArh)	NA	8.50	-12.96
	Electricity Cost (USD)	2.72	2.55	2.55
R17B	Active Energy (kWh)	28.78	26.91	26.94
	Reactive Energy (kVArh)	NA	-7.64	-7.95
	Electricity Cost (USD)	2.72	2.54	2.56
R18A	Active Energy (kWh)	33.36	31.31	31.39
	Reactive Energy (kVArh)	NA	-5.17	-12.47
	Electricity Cost (USD)	3.18	2.96	2.99
R18B	Active Energy (kWh)	24.21	22.46	22.53
	Reactive Energy (kVArh)	NA	-9.92	-16.73
	Electricity Cost (USD)	2.30	2.14	2.16
R18C	Active Energy (kWh)	3.98	35.76	35.86
	Reactive Energy (kVArh)	NA	-12.84	-14.35
	Electricity Cost (USD)	3.67	3.43	3.45
Total Active Energy (kWh)		398.02	373.26	373.89
Total Reactive Energy (kVArh)		NA	73.61	-68.66
Total Electricity Cost (USD)		37.78	35.34	35.48

Lastly, Table 2 summarizes the total active/reactive power consumption and total electricity costs for all consumers during a 24-hour period for the three different HEMSs: i) the conventional HEMS based on only the active power scheduling (HEMS 1), ii) the proposed voltage-reactive

power constrained HEMS (HEMS 2), and iii) HEMS 2 with voltage minimization term (HEMS 3). We can verify again from the table that HEMS 2 calculates less active energy and electricity cost than HEMS 1. We can conclude from this result that the proposed HEMS with the constraints associated with voltage and reactive power provides consumers with greater energy and electricity cost savings than conventional HEMS without these constraints. Further, we can verify from this table that compared to the results in HEMS 2, the voltage minimization in HEMS 3 does not yields the active energy and electricity saving whereas it results in a significant reduction of reactive energy. Here, positive reactive energy represents the reactive power consumed by the households, whereas negative reactive energy indicates reactive power being injected back to the grid. These different directions and amounts of the reactive energy consumption between HEMS 2 and HEMS 3 derive from the fact that reactive power contributes to achieve voltage minimization more significantly than active power.

To the best of the authors knowledge, this work is the first optimization framework of HEMS that is formulated with realistic distribution system models and operating conditions, including the constraints for active/reactive power flow and load consumption, voltage quality and voltage regulation, and three-phase unbalanced distribution systems with voltage-dependent load models. By incorporating the aforementioned constraints into the HEMS optimization framework, we verify the benefit of CVR in terms of the energy consumption of home appliances and the total electricity cost. The advantage and meaningful observations of the proposed approach can be summarized as follows:

- Comparing to the conventional HEMS method, the proposed HEMS approach can achieve a more energy saving by operating household appliances at a lower voltage level while maintaining the consumer's comfort level (i.e., preferred indoor temperature).
- The proposed HEMS approach ensures that the consumer voltage level maintains within its acceptable range through the coordination of the OLTC and smart inverters of DERs. However, the conventional HEMS approach may yields a voltage violation and incorrect voltage profile, consequently having a detrimental impact on home appliance' life time and undesired energy consumption schedule of home appliance.
- The proposed HEMS approach improves a distribution voltage profile along the entire distribution feeders in view of the active energy and electricity cost savings. This result derives from the fact that the performance of the proposed approach is marginally degraded with additional voltage minimization objective function and its corresponding constraints in term of active energy and electricity cost.

C. DISCUSSIONS

In this study, we assume that a single community HEMS can conduct both the energy consumption scheduling of smart households and voltage regulation in the entire LV distribution system. In addition, the operation of other controllable appliances (e.g., washing machine) and electric vehicles is excluded in the proposed HEMS algorithm. In these assumptions, a computational complexity of the community HEMS may increase significantly as the LV distribution system becomes larger with a larger number of home appliances and electric vehicles. Furthermore, consumers are at the risk of exposing their privacy to system operator or a third party due to a centralized data collection.

Nonetheless, we emphasize that our work is the first step toward developing the HEMS algorithm in realistic distribution system operating conditions and understanding the impact of voltage quality and reactive power on the HEMS performance. To resolve the computational complexity and consumer privacy issues, an important extension of our work would be to develop a cooperation framework between the distribution system operator using the VVO and the residential load aggregator using the HEMS including all types of controllable home appliances and referred to as a future work.

V. CONCLUSION

In this paper, a mixed-integer linear programming-based optimization algorithm was proposed for smart home energy management in three-phase unbalanced LV distribution systems. Compared to the existing home energy management optimization algorithms, the proposed algorithm minimizes the consumers' electricity cost within their comfort levels and maintains an acceptable voltage profile for consumers simultaneously by: i) optimally scheduling the active and reactive power consumption of unbalanced voltage-dependent household loads and distributed energy resource, and ii) dispatching active and/or reactive power from PV systems and ESSs together with the scheduling of the on-load tap changer tap position. Numerical examples simulated in a modified CIGRE LV distribution network confirm the effectiveness of the proposed algorithm in terms of the active/reactive power consumption, three-phase unbalanced voltage magnitudes, and total cost of electricity.

REFERENCES

[1] K. J. Chua, S. K. Chou, W. M. Yang, and J. Yan, "Achieving better energy-efficient air conditioning—A review of technologies and strategies," *Appl. Energy*, vol. 104, pp. 87–104, Apr. 2013.

[2] I. Ullah, N. Javaid, M. Imran, J. A. Khan, U. Qasim, M. Alnuem, and M. Bashir, "A survey of home energy management for residential customers," in *Proc. IEEE 29th Int. Conf. Adv. Inf. Netw. Appl.*, Gwangiu, South Korea, Mar. 2015, pp. 666–673.

[3] W. H. Kersting, *Distribution System Modeling and Analysis*. New York, NY, USA: CRC Press, 2017.

[4] A. Bokhari, A. Alkan, R. Dogan, M. Diaz-Aguiló, F. de León, D. Czarkowski, Z. Zabar, L. Birenbaum, A. Noel, and R. E. Uosef, "Experimental determination of the ZIP coefficients for modern residential, commercial, and industrial loads," *IEEE Trans. Power Del.*, vol. 29, no. 3, pp. 1372–1381, Jun. 2014.

[5] C. Long and L. F. Ochoa, "Voltage control of PV-rich LV networks: OLTC-fitted transformer and capacitor banks," *IEEE Trans. Power Syst.*, vol. 31, no. 5, pp. 4016–4025, Sep. 2016.

[6] L. Wang, F. Bai, R. Yan, and T. K. Saha, "Real-time coordinated voltage control of PV inverters and energy storage for weak networks with high PV penetration," *IEEE Trans. Smart Grid*, vol. 33, no. 3, pp. 3383–3395, May 2018.

[7] T. V. Dao, S. Chaitusaney, and H. T. N. Nguyen, "Linear least-squares method for conservation voltage reduction in distribution systems with photovoltaic inverters," *IEEE Trans. Smart Grid*, vol. 8, no. 3, pp. 1252–1263, May 2017.

[8] R. R. Jha, A. Dubey, C.-C. Liu, and K. P. Schneider, "Bi-level volt-VAR optimization to coordinate smart inverters with voltage control devices," *IEEE Trans. Power Syst.*, vol. 34, no. 3, pp. 1801–1813, May 2019.

[9] H. Ahmadi, J. R. Martí, and H. W. Dommel, "A framework for volt-VAR optimization in distribution systems," *IEEE Trans. Smart Grid*, vol. 6, no. 3, pp. 1473–1483, May 2015.

[10] Z. Wang, J. Wang, B. Chen, M. M. Begovic, and Y. He, "MPC-based voltage/var optimization for distribution circuits with distributed generators and exponential load models," *IEEE Trans. Smart Grid*, vol. 5, no. 5, pp. 2412–2420, Sep. 2014.

[11] B. A. Robbins and A. D. Domínguez-García, "Optimal reactive power dispatch for voltage regulation in unbalanced distribution systems," *IEEE Trans. Power Syst.*, vol. 31, no. 4, pp. 2903–2913, Jul. 2016.

[12] N. Daratha, B. Das, and J. Sharma, "Coordination between OLTC and SVC for voltage regulation in unbalanced distribution system distributed generation," *IEEE Trans. Power Syst.*, vol. 29, no. 1, pp. 289–299, Jan. 2014.

[13] F. Olivier, P. Aristidou, D. Ernst, and T. V. Cutsem, "Active management of low-voltage networks for mitigating overvoltages due to photovoltaic units," *IEEE Trans. Smart Grid*, vol. 7, no. 2, pp. 926–936, Mar. 2016.

[14] Z. Wang and J. Wang, "Review on implementation and assessment of conservation voltage reduction," *IEEE Trans. Power Sys.*, vol. 29, no. 3, pp. 1306–1315, May 2014.

[15] M. Pipattanasomporn, M. Kuzlu, and S. Rahman, "An algorithm for intelligent home energy management and demand response analysis," *IEEE Trans. Smart Grid*, vol. 3, no. 4, pp. 2166–2173, Dec. 2012.

[16] S. Shao, M. Pipattanasomporn, and S. Rahman, "Development of physical-based demand response-enabled residential load models," *IEEE Trans. Power Syst.*, vol. 28, no. 2, pp. 607–614, May 2013.

[17] D. T. Nguyen and L. B. Le, "Joint optimization of electric vehicle and home energy scheduling considering user comfort preference," *IEEE Trans. Smart Grid*, vol. 5, no. 1, pp. 188–199, Jan. 2014.

[18] C. Zhao, S. Dong, F. Li, and Y. Song, "Optimal home energy management system with mixed types of loads," *CSEE J. Power Energy Syst.*, vol. 1, no. 4, pp. 29–37, Dec. 2015.

[19] S. Althaher, P. Mancarella, and J. Mutale, "Automated demand response from home energy management system under dynamic pricing and power and comfort constraints," *IEEE Trans. Smart Grid*, vol. 6, no. 4, pp. 1874–1883, Jul. 2015.

[20] K. M. Tsui and S. C. Chan, "Demand response optimization for smart home scheduling under real-time pricing," *IEEE Trans. Smart Grid*, vol. 3, no. 4, pp. 1812–1821, Dec. 2012.

[21] N. G. Paterakis, O. Erdinç, I. N. Pappi, A. G. Bakirtzis, and J. P. S. Catalão, "Coordinated operation of a neighborhood of smart households comprising electric vehicles, energy storage and distributed generation," *IEEE Trans. Smart Grid.*, vol. 7, no. 6, pp. 2736–2747, Nov. 2016.

[22] O. Erdinc, N. G. Paterakis, T. D. P. Mendes, A. G. Bakirtzis, and J. P. S. Catalão, "Smart household operation considering bi-directional EV and ESS utilization by real-time pricing-based DR," *IEEE Trans. Smart Grid*, vol. 6, no. 3, pp. 1281–1291, May 2015.

[23] S. Lee, B. Kwon, and S. Lee, "Joint energy management system of electric supply and demand in houses and buildings," *IEEE Trans. Power Syst.*, vol. 29, no. 6, pp. 2804–2812, Nov. 2014.

[24] F. Luo, G. Ranzi, C. Wan, Z. Xu, and Z. Y. Dong, "A multistage home energy management system with residential photovoltaic penetration," *IEEE Trans. Ind. Informat.*, vol. 15, no. 1, pp. 116–126, Jan. 2019.

[25] X. Ran and S. Leng, "Enhanced robust index model for load scheduling of a home energy local network with a load shifting strategy," *IEEE Access.*, vol. 7, pp. 19943–19953, 2019. doi: 10.1109/ACCESS.2018.2889762.

[26] J. Wang, P. Li, K. Fang, and Y. Zhou, "Robust optimization for household load scheduling with uncertain parameters," *Appl. Sci.*, vol. 8, no. 4, p. 575, Apr. 2018.

[27] M. Rastegar, M. Fotuhi-Firuzabad, and M. Moeini-Aghtai, "Developing a two-level framework for residential energy management," *IEEE Trans. Smart Grid*, vol. 9, no. 3, pp. 1707–1717, May 2018.

[28] I.-Y. Joo and D.-H. Choi, "Distributed optimization framework for energy management of multiple smart homes with distributed energy resources," *IEEE Access.*, vol. 5, pp. 2169–3536, 2017.

[29] H. Shareef, M. S. Ahmed, A. Mohamed, and E. A. Hassan, "Review on home energy management system considering demand responses, smart technologies, and intelligent controllers," *IEEE Access.*, vol. 6, pp. 24498–24509, 2018.

[30] M. Ruth, A. Pratt, M. Lunacek, S. Mittal, H. Wu, and W. Jones, "Effects of home energy management systems on distribution utilities and feeders under various market structures," in *Proc. 23rd Int. Conf. Electr. Distrib.*, Jun. 2015, pp. 666–673.

[31] S. Sekizaki, I. Nishizaki, and T. Hayashida, "Impact of retailer and consumer behavior on voltage in distribution network under liberalization of electricity retail market," *Electr. Eng. Jpn.*, vol. 194, no. 4, pp. 27–41, Mar. 2015.

[32] O. Elma and U. S. Selamogullari, "A new home energy management algorithm with voltage control in a smart home environment," *Energy*, vol. 91, pp. 720–731, Nov. 2015.

[33] F. A. Rahiman, H. H. Zeineldin, V. Khadkikar, S. W. Kennedy, and V. R. Pandi, "Demand response mismatch (DRM): Concept, impact analysis, and solution," *IEEE Trans. Smart Grid.*, vol. 5, no. 4, pp. 1734–1743, Jul. 2014.

[34] B. Chen, C. Chen, J. Wang, and K. L. Butler-Purry, "Sequential service restoration for unbalanced distribution systems and microgrids," *IEEE Trans. Power Syst.*, vol. 33, no. 2, pp. 1507–1520, Mar. 2018.

[35] G. P. McCormick, "Computability of global solutions to factorable nonconvex programs: Part I—Convex underestimating problems," *Math. Program.*, vol. 10, no. 1, pp. 147–175, Dec. 1976.

[36] K. Strunz, "Benchmark systems for network integration of renewable and distributed energy resources," CIGRE Task Force, Paris, France, Tech. Rep. 575, Apr. 2014.

[37] D. Mak and D.-H. Choi, "Hierarchical look-ahead conservation voltage reduction framework considering distributed energy resources and demand reduction," *Energies*, vol. 11, no. 12, p. 3250, Nov. 2018.

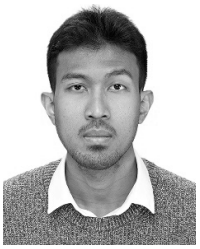

DAVYE MAK (S'17) received the bachelor's degree in electrical and electronics engineering from the Institute of Technology of Cambodia (ITC), Phnom Penh, Cambodia, and the M.E. degree in electric energy from Chung-Ang University, Seoul, South Korea, where he is currently pursuing the Ph.D. degree. His current research interests include advanced volt-var control and optimization, and home energy management system in smart grid.

DAE-HYUN CHOI (S'10–M'17) received the B.S. degree in electrical engineering from Korea University, Seoul, South Korea, in 2002, and the M.Sc. and Ph.D. degrees in electrical and computer engineering from Texas A&M University, College Station, TX, USA, in 2008 and 2014, respectively. From 2002 to 2006, he was a Researcher with the Korea Telecom (KT), Seoul, where he worked on designing and implementing home network systems. From 2014 to 2015, he was a Senior Researcher with LG Electronics, Seoul, where he developed home energy management systems. He is currently an Associate Professor with the School of Electrical and Electronics Engineering, Chung-Ang University, Seoul. His research interests include power system state estimation, electricity markets, the cyber-physical security of smart grids, and the theory and application of cyber-physical energy systems. He received the Best Paper Award at the 2012 IEEE Third International Conference on Smart Grid Communications (SmartGridComm), Tainan, Taiwan.